1   **FTO suppresses STAT3 activation and modulates proinflammatory interferon-stimulated**

2   **gene expression**

3

4   Michael J. McFadden[1, a*], Matthew T. Sacco[1*], Kristen A. Murphy[1], Moonhee Park[1], Nandan S.

5   Gokhale[2], Kim Y. Somfleth[2], Stacy M. Horner[†1,3]

6

7   Affiliations:

8   [1]   Department of Molecular Genetics and Microbiology, Duke University Medical Center,

9   Durham, NC 27710, USA.

10   Michael J. McFadden; mcfaddmj@umich.edu, Matthew T. Sacco;

11   matthew.sacco@duke.edu, Kristen A. Murphy; kristen.a.murphy@duke.edu, Moonhee

12   Park; moonhee.park@duke.edu, Stacy M. Horner; stacy.horner@duke.edu

13   [2]   Department of Immunology, University of Washington, Seattle, WA 98109, USA.

14   Nandan S. Gokhale; ngokhale@uw.edu, Kim Y. Somfleth; ksomf@uw.edu

15   [3]   Department of Medicine, Duke University Medical Center, Durham, NC 27710, USA.

16

17

18   Current address:

19   [a]   Department of Microbiology and Immunology, University of Michigan, Ann Arbor, MI

20   48109, USA.

21

22

23

24

25   * These authors contributed equally

26

27   [†] Corresponding author

28   Correspondence to Stacy M. Horner (stacy.horner@duke.edu)

29   **Abstract**

30   Signaling initiated by type I interferon (IFN) results in the induction of hundreds of IFN-

31   stimulated genes (ISGs). The type I IFN response is important for antiviral restriction, but aberrant

32   activation of this response can lead to inflammation and autoimmunity. Regulation of this

33   response is incompletely understood. We previously reported that the mRNA modification m^6A

34   and its deposition enzymes, METTL3 and METTL14 (METTL3/14), promote the type I IFN

35   response by directly modifying the mRNA of a subset of ISGs to enhance their translation. Here,

36   we determined the role of the RNA demethylase FTO in the type I IFN response. FTO, which can

37   remove either m^6A or the cap-adjacent m^6Am RNA modifications, has previously been associated

38   with obesity and body mass index, type 2 diabetes, cardiovascular disease, and inflammation.

39   We found that FTO suppresses the transcription of a distinct set of ISGs, including many known

40   pro-inflammatory genes, and that this regulation is not through the actions of FTO on m^6Am.

41   Further, we found that depletion of FTO led to activation of STAT3, a transcription factor that

42   mediates responses to various cytokines, but whose role in the type I IFN response is not well

43   understood. This activation of STAT3 increased the expression of a subset of ISGs. Importantly,

44   this increased ISG induction resulting from FTO depletion was partially ablated by depletion of

45   STAT3. Together, these results reveal that FTO negatively regulates STAT3-mediated signaling

46   that induces proinflammatory ISGs during the IFN response, highlighting an important role for

47   FTO in suppression of inflammatory genes.

48

49   **Keywords:** Fat mass and obesity-associated (FTO); N6-methyladenosine (m^6A); Interferon (IFN);

50   Interferon-stimulated gene (ISG); Inflammation

51

52   **Introduction**

53   The type I interferon (IFN) response induces the expression of hundreds of IFN-stimulated

54   genes (ISGs), many of which have antiviral and proinflammatory functions, and thus is crucial for

55   the early response to viral infection [1]. Type I IFNs signal through a dimeric receptor composed

56   of IFNAR1 and IFNAR2 to activate the transcription factors STAT1 and STAT2, which

57   heterodimerize with IRF9 to form the transcription factor complex ISGF3 [2]. ISGF3 then binds to

58   the promoters of ISGs to induce their transcription, resulting in the establishment an antiviral

59   cellular state [3]. While transcriptional induction of ISGs by ISGF3 is the primary driver of the type

60   I IFN response, regulation of this response by other transcription factors or by post-transcriptional

61   controls is incompletely understood. Specifically, the functions of the transcription factor STAT3

62   in the type I IFN response are not clear, although it has been shown to have functions either in

2

63   suppressing this response or promoting the expression of certain ISGs, likely in a cell type-specific

64   fashion [4]. We previously established that the addition of the mRNA modification m^6A to a subset

65   of ISGs by the m^6A-methyltransferase complex proteins METTL3 and METTL14 (METTL3/14)

66   increases their translation by recruiting the m^6A-binding protein YTHDF1 and that this promotes

67   an antiviral cellular state [5]. However, the role of the m^6A demethylase FTO in the type I IFN

68   response has not yet been described. The functions of FTO are important for several aspects of

69   human health, and genetic variants of this gene are associated with obesity and body mass index,

70   type 2 diabetes, cardiovascular disease, and inflammation [6-9]. Despite its essential functions

71   for human development and health [10], the mechanisms by which FTO regulates these biological

72   processes are incompletely understood.

73   A major molecular function of FTO, which has sequence homology to alpha-ketoglutarate

74   oxygenase enzymes such as the AlkB homolog family (ALKBH) proteins, is RNA demethylation

75   [11]. Importantly, FTO has been shown to be involved in the demethylation of both m^6A [12], a

76   function shared by ALKBH5 [13], and the cap-adjacent m^6Am modification [14]. m^6A is deposited

77   by a complex of proteins, including METTL3/14 and others [15], and can regulate many aspects

78   of RNA metabolism, including degradation and translation, among other processes [16-19]. m^6Am

79   addition is catalyzed by the enzyme PCIF1 at the first transcribed nucleotide in an mRNA and

80   may be involved in regulating mRNA stability and translation [20-22]. Through its RNA

81   demethylase functions, FTO can regulate many cellular and biological processes, including

82   neurogenesis, dopamine signaling and appetite regulation, adipogenesis, oncogenesis, and viral

83   infection [23-29]. Interestingly, FTO depletion was recently shown to sensitize melanoma cells to

84   IFN-γ treatment, suggesting a role for FTO in the response to IFNs [28]. Further, FTO has been

85   shown to regulate infection by a number of viruses, presumably by demethylating viral RNA [29],

86   but its role in regulation of host responses to viral infection has not been elucidated. Therefore,

87   we sought to define the role of FTO in the type I IFN response.

88   Here, we found that depletion of FTO results in increased production of a subset of ISGs.

89   However, whereas METTL3/14 promotes the translation of a subset of ISGs without affecting their

90   mRNA levels [5], FTO regulates a distinct subset of ISGs at the mRNA level. By labeling nascent

91   RNA, we found that FTO inhibits the transcription of these ISGs and that FTO-depleted cells are

92   primed to respond to type I IFN. FTO regulation of ISGs is not through demethylation of m^6Am,

93   as deletion of the m^6Am writer enzyme PCIF1 did not impact the phenotypic effect of FTO

94   depletion on ISG expression. Interestingly, we found that FTO depletion results in increased

95   phosphorylation and thus activation of transcription factor STAT3. Additionally, STAT3 activation

96   through treatment with the cytokine IL6 or expression of the *Salmonella* effector protein SarA,

3

97 known to induce STAT3 phosphorylation, recapitulated the phenotypic effects of STAT3 activation

98 by FTO depletion [30, 31], suggesting that suppression of STAT3 activation by FTO represses

99 transcription of a specific subset of ISGs. In support of this hypothesis, depletion of STAT3 led to

100 partial ablation of FTO-mediated suppression of ISG induction. Taken together, these results

101 reveal a novel role for FTO in the transcriptional suppression of STAT3-regulated ISGs, which

102 has important implications for our understanding of the role of FTO in disease.

103

104 **Results**

105 **FTO regulates the mRNA expression of a subset of ISGs.**

106 Having previously shown that the m^6A-methyltransferase complex proteins METTL3/14

107 promote the translation of specific ISGs via the addition of m^6A to these ISGs [5], we hypothesized

108 that the major m^6A-demethylase FTO would suppress the translation of these ISGs by removal of

109 m^6A. To test this hypothesis, we used siRNAs to deplete METTL3/14 or FTO in Huh7 cells and

110 induced the expression of ISGs by treatment with IFN-β, a type I IFN. Similar to our previous

111 results, depletion of METTL3/14 resulted in reduced protein levels of IFITM1, GBP1, IFIT3, and

112 MX1 [5]. Depletion of FTO showed the opposite result in that its depletion resulted in increased

113 protein expression of the METTL3/14-regulated ISGs, expect for MX1 whose expression was only

114 modestly affected by METTL3/14 depletion and not altered by FTO depletion (Figure 1A). As

115 before, the ISGs ISG15 and EIF2AK2 were unaffected by METTL3/14 depletion, and here we

116 also found that their IFN-induced expression was unaffected by FTO depletion (Figure 1A). We

117 next determined whether FTO depletion changed the mRNA induction of these ISGs.

118 Interestingly, while METTL3/14 depletion did not impact the mRNA levels of these ISGs, as

119 expected [5], FTO depletion did increase the mRNA levels of the regulated ISGs, including

120 *IFITM1*, *GBP1*, and *IFIT3* (Figure 1B). These results show that FTO negatively regulates specific

121 ISGs at the mRNA level. Thus, the mechanism underlying the regulatory role of FTO on ISGs is

122 distinct from METTL3/14.

123
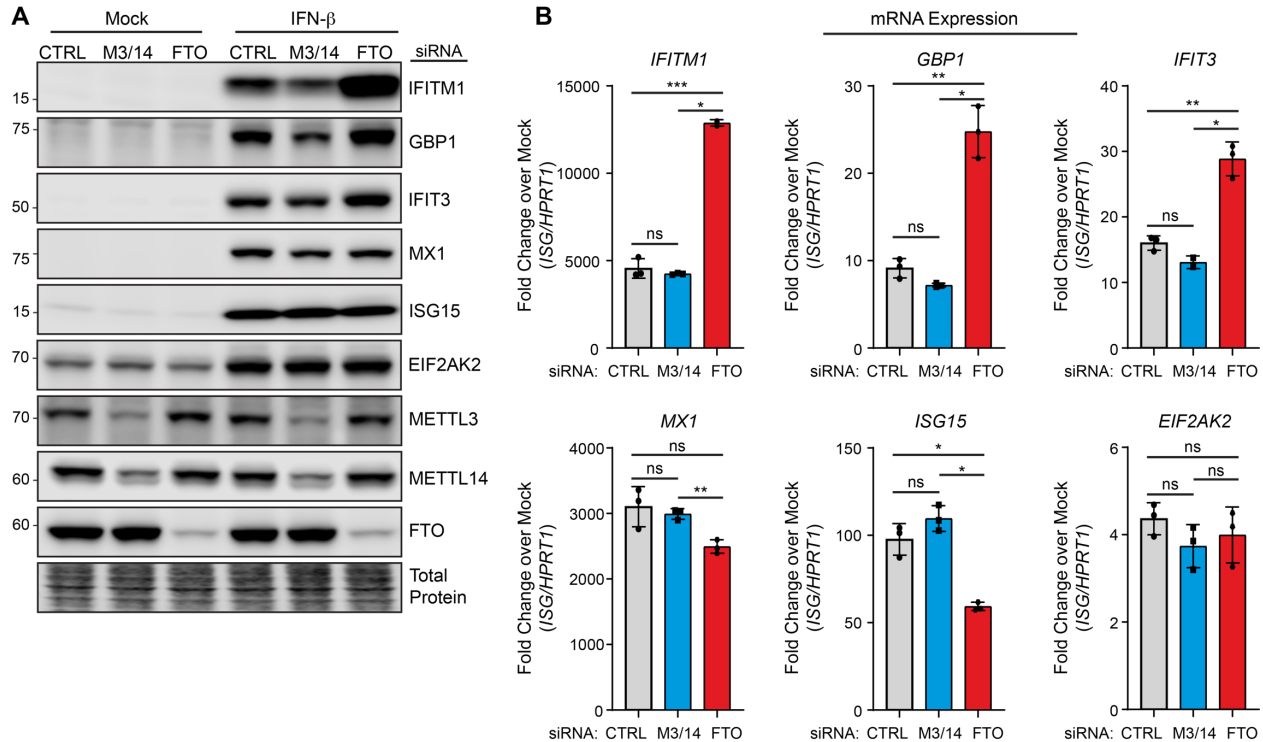
Figure 1: FTO regulates the mRNA expression of a subset of ISGs. (A) Immunoblot analysis of extracts from Huh7 cells transfected with siRNAs to control (CTRL), METTL3/14 (M3/14), or FTO prior to mock or IFN-β (12 h) treatment. Data are representative of 3 biological experiments. **(B)** RT-qPCR analysis of ISG induction normalized to *HPRT1* following IFN-β treatment (12 hours) of Huh7 cells treated with non-targeting control (CTRL) or METTL3/14 siRNA plotted as fold change over mock treatment for each ISG. Values are the mean ± SD of 3 technical replicates, representative of 3 biological experiments. * $p < 0.05$, ** $p < 0.01$, *** $p < 0.005$ by one way ANOVA with Dunnett's multiple comparisons test.

FTO regulates the transcription of certain ISGs.

To determine how FTO regulates the mRNA expression of ISGs, we pulsed siCTRL, siMETTL3/14, or siFTO-treated cells with 4-thiouridine (4-sU) and IFN-β for 1 hour to metabolically label nascent transcripts produced by IFN stimulation. We then purified the nascent RNA and performed RT-qPCR to quantify relative transcription. These experiments revealed that depletion of FTO led to a marked increase of the transcription of the FTO-regulated ISG *IFITM1* during the pulse. Interestingly, the transcription of the non-FTO-regulated ISGs *ISG15* and *EIF2AK2* were also slightly increased by FTO depletion (Figure 2A). METTL3/14 depletion did not affect the transcription of these ISGs nor a known m6A-modified gene, *CREBBP*, whose stability is regulated by m6A [16] (Figure 2A). Next, to determine how FTO regulates the transcription of ISGs over time, we performed the 4-sU and IFN-β pulses at both 1 and 12 hours

5

144   in siRNA-treated cells and quantified the transcription of a broader set of ISGs by RT-qPCR

145   (Figure 2B). Similar to the results shown in Figure 2A, following the 1 hour 4-sU and IFN-β pulses

146   nearly all ISGs tested (*IFITM1, GBP1, IFIT3, MX1, ISG15,* and *EIF2AK2*) displayed some

147   increased transcription following FTO depletion. However, following the 12 hour 4-sU and IFN-β

148   pulses, only *IFITM1, GBP1, and IFIT3* still had increased transcription, while the non-FTO

149   regulated ISGs *MX1, ISG15,* and *EIF2AK2* did not (Figure 1B; Figure 2B). These data indicate

150   that FTO depletion primes cells to respond to IFN-β, as they transcribe ISGs more rapidly, but

151   this early transcriptional upregulation only persist for a subset of ISGs.

152
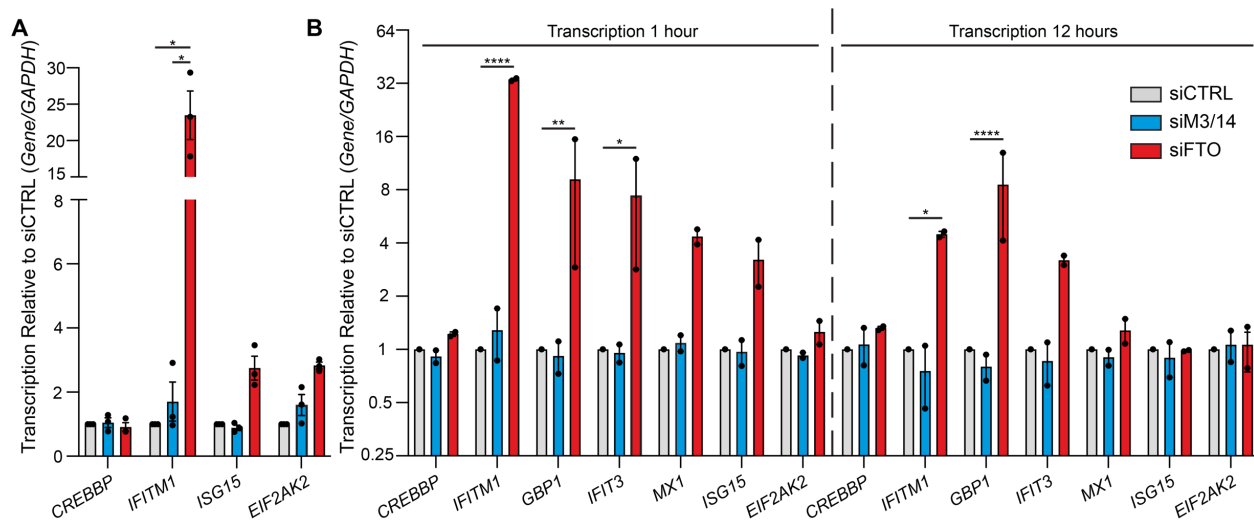
153   **Figure 2: FTO regulates the transcription of ISGs. (A-B)** Relative transcription analysis of
154   Huh7 cells treated with siRNAs to control (CTRL), METTL3/14 (M3/14), or FTO prior to mock or
155   IFN-β treatment + 4-sU pulse labeling for 1 hour (A) or 1 and 12 hours (B). Values are the mean
156   ± SEM of 3 (A) or 2 (B) biological experiments. * P < 0.01; all other comparisons not significant
157   (P > 0.05) by 2-way ANOVA with Tukey's multiple comparisons.

158

159   **FTO regulation of ISGs occurs independently of m⁶Am.**

160   FTO can catalyze the removal of both m^6A and m^6Am [12, 14]. To determine if FTO acts

161   on m^6Am or on m^6A to suppress the expression of ISGs, we removed expression of the m^6Am-

162   methylase PCIF1 [20, 21] using PCIF1 knockout cells generated by CRISPR/Cas9 [20]. Then, we

163   tested if loss of m^6Am by PCIF1 knockout could abrogate suppression of ISGs by FTO. To do

164   this, we depleted FTO in either parental 293T cells or in two independent clonal cell lines in which

165   the m^6Am-methylase PCIF1 was removed by CRISPR/Cas9 [20]. Following IFN-β treatment for

166   12 hours, we measured the expression of the FTO-regulated ISGs IFITM1 and IFIT3 by

167   immunoblot and found that the upregulation of IFITM1 and IFIT3 seen upon FTO depletion was

168   not altered by loss of PCIF1 expression (Figure 3A). These results reveal that FTO regulation of

169   ISGs does not occur through m^{6}Am modification of RNAs.
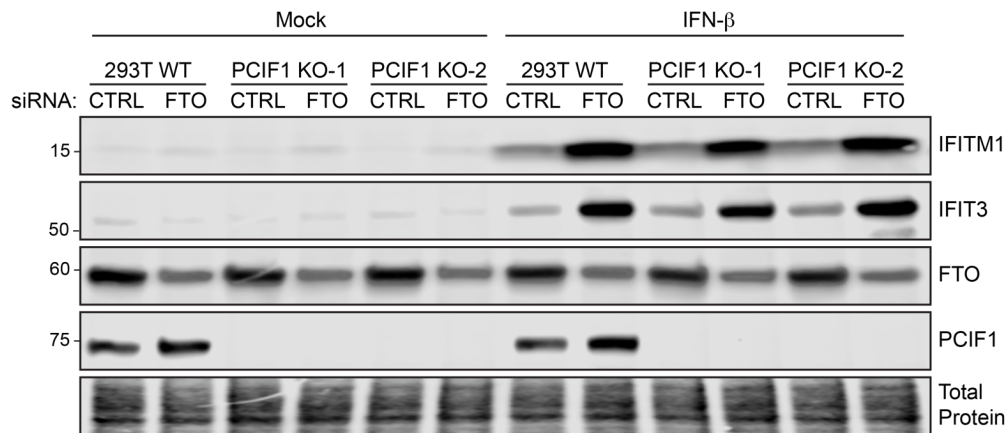

170

171   **Figure 3: FTO regulation of ISGs occurs independently of m^{6}Am.** Immunoblot analysis of
172   extracts from wild-type (WT) 293T cells or two clonal PCIF1 knockout cell lines transfected with
173   siRNAs to control (CTRL) or FTO prior to mock or IFN-β (12 h) treatment. Data are representative
174   of 3 biological experiments.

175   **FTO suppresses inflammatory gene expression.**

176   Having determined that FTO regulates the transcription of certain ISGs, we next sought

177   to more broadly characterize the regulatory role of FTO during the type I IFN response. Using

178   RNA-seq, we profiled gene expression in FTO-depleted cells, following mock treatment or IFN-β

179   stimulation (8 hours) (Table S1). Genes regulated by FTO in mock-treated cells were enriched in

180   biological categories such as RNA metabolism and gene expression, supporting the known role

181   of FTO in RNA regulation, as well as immune categories such as response to IFN-γ and response

182   to external biotic stimulus (Table S2.1) [12]. Gene ontology analysis of the genes significantly

183   regulated by FTO (adjusted P < 0.01) during the IFN response revealed that FTO-regulated genes

184   are enriched in biological categories related to immunity, defense responses, and cytokines

185   (Figure 4A; Table S2.2. To determine the effect of FTO depletion on the IFN-induced expression

186   of ISGs, we profiled the 300 most highly-induced ISGs that we had previously defined [5] (Figure

187   4B; Table S1.1) and found that FTO depletion led to increased expression of a subset of these

188   ISGs (Figure 4C; Table S1.2). Indeed, 140 of these ISGs were significantly regulated by FTO

189   (adjusted P<0.01) and of these 140, nearly all (136) were upregulated following FTO depletion,

190   confirming that FTO is a suppressor of a distinct set of ISGs. While these IGSs are also induced

191   following FTO depletion in the absence of IFN treatment (Figure 4D; Table S1.3), these effects

192   were generally exacerbated by IFN-β treatment, as seen in a heatmap of the top 50 most highly-

193   induced FTO-regulated ISGs (Figure 4E), further supporting the idea that FTO-depleted cells are

194 primed to respond to IFN-β. The ISGs most highly upregulated by FTO depletion include the

195 proinflammatory chemokines *CXCL10* and *CXCL11* (Figure 4A). Indeed, our analysis of

196 proinflammatory gene expression revealed that FTO depletion generally led to an upregulation of

197 proinflammatory gene expression [32], with strong upregulation of the proinflammatory cytokines

198 *TNF* and *IL6* and the proinflammatory chemokines *CXCL9, CXCL10,* and *CXCL11* (Figure 4F).

199 Together, these results reveal that FTO negatively regulates a subset of ISGs, including many

200 proinflammatory genes.
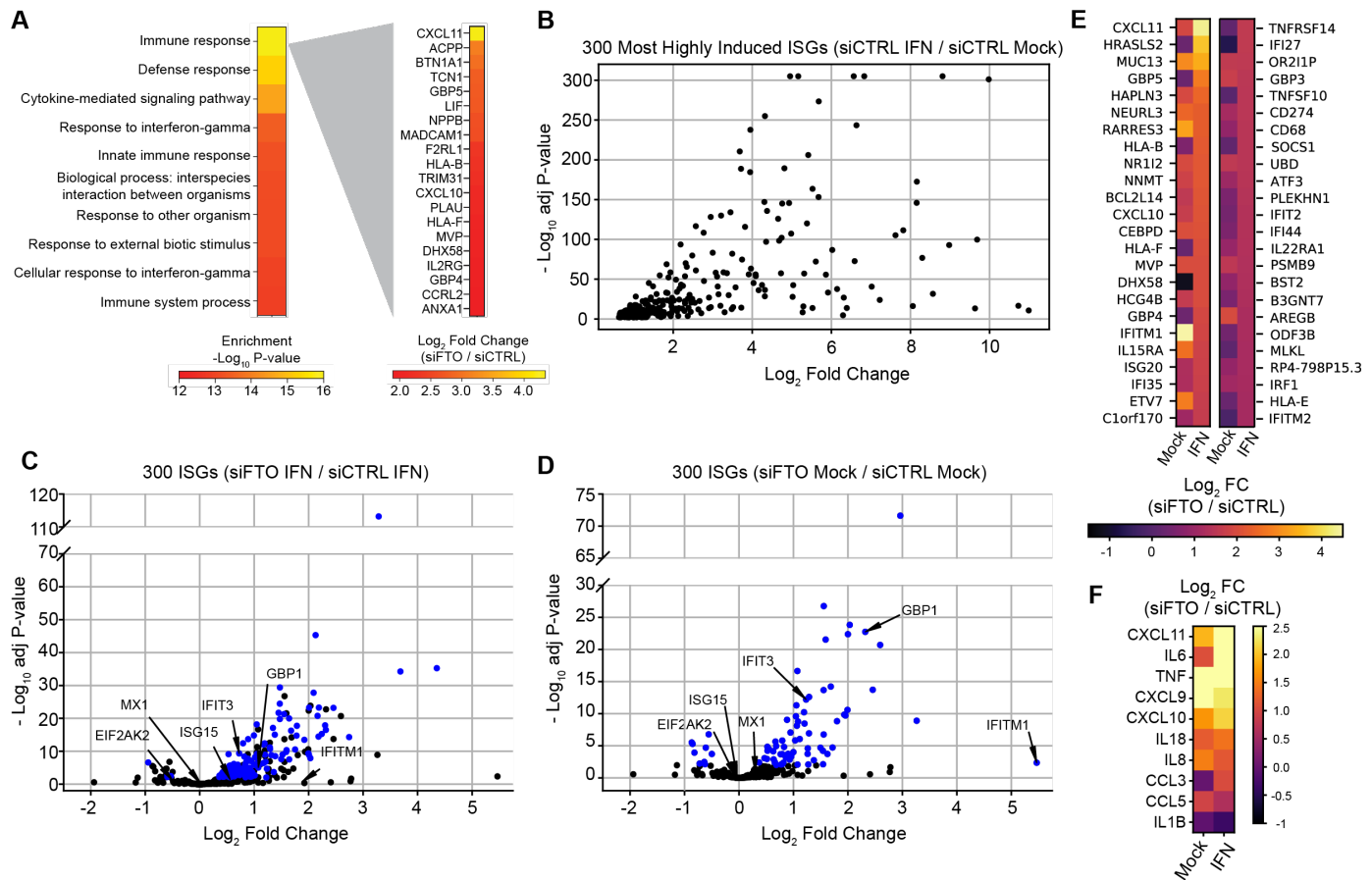
201

202 **Figure 4: FTO suppresses inflammatory gene expression.** RNA-seq analysis of Huh7 cells
203 treated with siRNAs to control (CTRL) or FTO (36 h), followed by mock or IFN-β treatment (8 h).
204 **(A)** Gene ontology analysis of differentially expressed genes in IFN-β-treated cells (siFTO /
205 siCTRL). Left panel shows biological categories and right panel shows differentially expressed
206 genes within the immune response category. **(B-D)** Volcano plots of the 300 most highly-
207 induced ISGs (adjP<0.01; basemean > 50) (A), and the effect of FTO depletion on these 300
208 ISGs (siFTO / siCTRL) in IFN-β treated cells (B), or mock-treated cells (C). **(E)** Heatmap of the
209 effect of FTO depletion on the 50 most induced ISGs (siFTO / siCTRL) following mock and IFN-
210 β treatment. **(F)** Heatmap of the effect of FTO depletion on canonical proinflammatory cytokines
211 and chemokines (siFTO / siCTRL).

212 **FTO suppresses STAT3 activation.**

213   Having found that FTO suppresses the transcription of only a subset of ISGs and that
214 FTO-depleted cells are primed to respond to type I IFN, we hypothesized that FTO may regulate
215 these ISGs through a transcription factor other than the canonical ISGF3 complex of STAT1,
216 STAT2, and IRF9 [2]. Interestingly, FTO has previously been found to regulate the activation of
217 the transcription factor STAT3 [33], which can drive transcriptional induction of proinflammatory
218 gene expression and possibly certain ISGs [34, 35]. The activation of STAT3 requires its
219 phosphorylation at the tyrosine 705 (Y705) residue [36]. Thus, to test if FTO negatively regulates
220 STAT3 activation we measured phosphorylation of STAT3 at Y705 in METTL3/14- or FTO-
221 depleted Huh7 cells by immunoblot. FTO depletion, but not METTL3/14 depletion, led to an
222 increase in STAT3 phosphorylation, and this increase was similar in the presence or absence of
223 IFN (Figure 5A). To determine if STAT3 activation is sufficient to induce FTO-regulated ISGs, we
224 treated Huh7 cells with IL-6, which induces Y705 phosphorylation of STAT3 [30]. While IL-6 did
225 induce Y705 phosphorylation of STAT3, it did not induce ISG expression, as measured by
226 immunoblot. However, in conjunction with IFN-β treatment, IL-6 did modestly enhance the
227 expression of the FTO-regulated ISGs IFITM1 and IFIT3, but not ISG15 and EIF2AK2. These
228 data suggest in the presence of IFN-β, activation of STAT3 can recapitulate the effect of FTO
229 depletion on ISG expression (Figure 5B). Additionally, STAT3 activation in Huh7 cells by
230 expression of the *Salmonella* effector protein SarA, which is known to activate STAT3 [31],
231 resulted in increased expression of IFITM1 and IFIT3, but not ISG15 and EIF2AK2, following both
232 mock and IFN-β treatment (Figure 5C), supporting our finding that STAT3 activation can regulate
233 ISGs in a similar fashion to FTO depletion during the IFN response. To determine whether STAT3
234 activation is responsible for the upregulation of ISGs that results from FTO depletion, we co-
235 depleted FTO and STAT3 in Huh7 cells using siRNA. Depletion of STAT3 alone reduced the
236 expression of IFITM1 and IFIT3, but not ISG15 and EIF2AK2 (Figure 5D). Importantly, STAT3
237 depletion also partially ablated the effect of FTO depletion on IFITM1 and IFIT3 (Figure 5D).
238 Together, these data reveal that FTO suppresses the expression of a subset of ISGs by inhibiting
239 STAT3 activation.

9
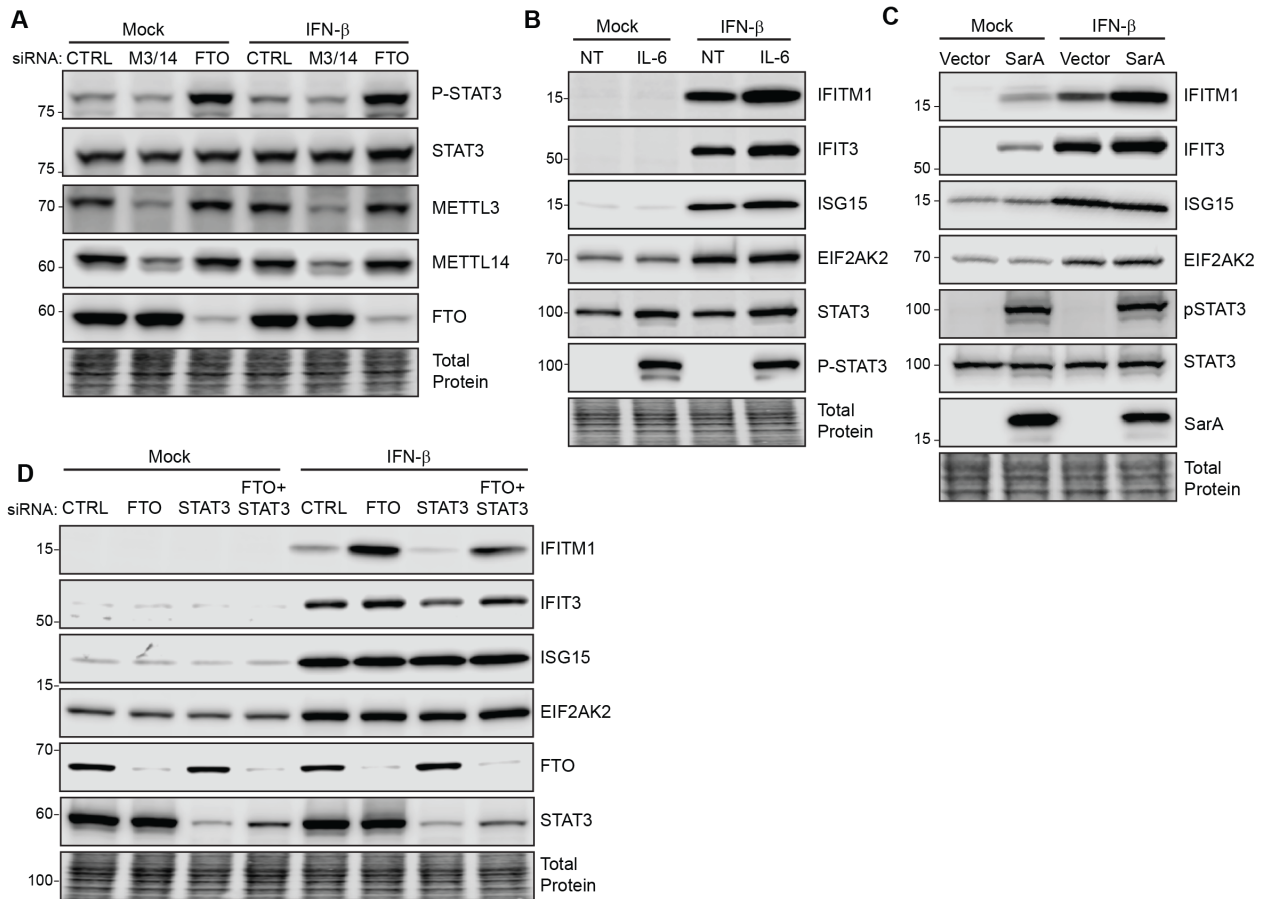
Figure 5: FTO suppresses STAT3 activation. (A) Immunoblot analysis of extracts from Huh7 cells transfected with siRNAs to control (CTRL), METTL3/14 (M3/14), or FTO prior to mock or IFN-β (12 h) treatment. **(B)** Immunoblot analysis of extracts from Huh7 treated with mock or IFN-β plus IL-6 or no treatment (NT) for 12 h. **(C)** Immunoblot analysis of extracts from Huh7 cells expressing SarA or vector (16 h), followed by IFN-β (12 h) treatment. **(D)** Immunoblot analysis of extracts from Huh7 cells transfected with siRNAs to control (CTRL), STAT3, FTO, or FTO and STAT3 prior to mock or IFN-β (12 h) treatment. Data in A-D are representative of 3 biological experiments.

Discussion

We previously found that METTL3/14 and m6A facilitate the translation of a subset of m6A-modified ISGs [5]. Given the m6A and m6Am demethylase activities of FTO, we hypothesized that FTO could inhibit the translation of ISGs through demethylation of these modifications on the transcripts of ISGs. However, here, we found that FTO suppresses signaling and transcriptional activation of a subset of ISGs, including many that encode proinflammatory factors. This regulatory function of FTO does not occur through its effect on m6Am, as the regulatory effect of FTO on ISGs was intact in cells that do not express the m6Am methyltransferase PCIF1. As

10

258   genetic ablation of METTL3 is not tolerated by Huh7 and other cancer cell lines [37], we were
259   unable to determine whether FTO regulation of ISGs is dependent on METTL3-mediated m^{6}A
260   modifications. However, we did find that the major mechanism by which FTO suppressed ISG
261   expression was through its negative regulation of STAT3 activation, which induces specific
262   classes of ISGs (Figure 5). Therefore, our data suggest that active STAT3 may act synergistically
263   with ISGF3 at the promoters of certain ISGs. Given the association of FTO variants with
264   inflammation-related diseases [6-9], these results increase our knowledge of the molecular roles
265   of FTO in human diseases driven by inflammation. Additionally, our work establishes a novel role
266   for FTO as a suppressor of ISGs, and thus defines a new control for the IFN response.

267   The role of STAT3 in the type I IFN response is unclear. The type I IFN response is
268   typically driven by the ISGF3 transcription factor complex, which is composed of STAT1, STAT2,
269   and IRF9. While this complex does not canonically include STAT3, STAT3 has been shown to be
270   activated by type I IFN in certain cell types [4]. However, most functions of type I IFN signaling,
271   such as antiviral gene expression and immune cell development, are independent of STAT3 [38-
272   40]. In cell types in which STAT3 is activated in response to type I IFN, it has been show to
273   function as either a positive or negative regulator of type I IFN signaling [4, 35, 41]. The
274   mechanisms by which STAT3 may repress type I IFN signaling include sequestration of STAT1
275   [41], cooperation with repressor proteins such as PLSCR2 [42], or induction of negative regulators
276   of the JAK-STAT pathway, such as SOCS family proteins [43]. However, in addition to these
277   repressive roles, STAT3 has been shown to support or enhance the expression of certain ISGs,
278   such as OAS and MX2 [41], as well as CXCL11 [35], which we found to be among the highest
279   upregulated genes by FTO depletion. Interestingly, in our experiments, STAT3 phosphorylation
280   was not induced by IFN-β treatment alone, but known STAT3 phosphorylation activators such as
281   IL-6 and the Salmonella effector protein SarA induced expression of ISGs that are also increased
282   by FTO depletion (Figure 5). These data suggest that STAT3 can activate the transcription of a
283   subset of ISGs, as well as act synergistically with the ISGF3 transcription factor complex
284   canonically activated by type I IFN to enhance the expression of these ISGs. As such, STAT3
285   may be responsible for the transcriptional priming of ISGs that we observed following FTO
286   depletion (Figure 2), although this effect seems to be transient for many ISGs, perhaps due to
287   their eventual negative regulation [44]. Whether STAT3 directly promotes ISG transcription by
288   binding to the promoters of these genes or by an indirect mechanism, as well as determining the
289   cell type specificity of this STAT3-mediated regulation, will be an interesting direction for future
290   research.

291   Previous studies have reported conflicting roles of FTO in regulation of STAT3 activation.
292   In agreement with our findings, FTO overexpression in liver cells can decrease phosphorylation
293   of STAT3 at Y705 and reduce its nuclear localization [33], suggesting that FTO suppresses
294   STAT3 activation. However, other studies in adipocytes have suggested that FTO increases
295   STAT3 activation by stabilizing the mRNA of *JAK2,* which encodes a known STAT3 kinase, to
296   induce STAT3 phosphorylation at Y705 [45]. Therefore, molecular regulation between FTO and
297   STAT3 is complex and may differ in specific cell types. However, given the role of FTO in
298   regulation of mRNA expression, it is likely that FTO regulates the expression of one or more
299   factors that govern STAT3 Y705 phosphorylation through regulation of m^6A on specific transcripts.
300   Indeed, our RNA-seq data revealed that *JAK2* mRNA expression was upregulated following FTO
301   depletion. As JAK2 encodes a kinase that can phosphorylate STAT3 at Y705 in response to IL6
302   [46], it is possible that upregulation of JAK2 expression is responsible for the increase in STAT3
303   phosphorylation and activation observed following FTO depletion. While the m^6Am demethylase
304   function of FTO is not required for its regulation of ISGs, it is possible that it regulates one or
305   several factors controlling STAT3 activation, such as JAK2, in an m^6A demethylase-dependent
306   fashion. Indeed, we previously found that JAK2 mRNA is m^6A-modified during the type I IFN
307   response [5]. However, as FTO depletion may regulate the expression of multiple kinases or
308   phosphatases that control STAT3 phosphorylation [47], additional targeted studies will be
309   required for a more complete understanding of the mechanisms by which FTO regulates STAT3
310   activation.

311   In summary, we found that FTO acts as a transcriptional suppressor of a subset of ISGs,
312   including many genes encoding proinflammatory factors. This function of FTO is independent of
313   its role as an m^6Am demethylase and is mediated at least partially by suppression of STAT3
314   activation. These results reveal a novel regulatory control over the type I IFN response and shed
315   additional light on the molecular role of FTO in regulation of immune gene expression. As FTO
316   and its substrate modifications m^6A and m^6Am can regulate viral infection through their effects on
317   both viral and host RNAs [29, 48, 49], these results will help shape our understanding of the
318   functions of FTO during viral infection. While previous studies have described associations
319   between FTO and immune-related gene expression [27, 50], our work sheds additional light on
320   the mechanisms by which FTO influences innate immune and proinflammatory gene expression.
321   Further, this molecular role of FTO could have important implications for our understanding of the
322   role of FTO in inflammation-related diseases, such as obesity and cancer. Thus, further
323   exploration of the relationship between FTO, STAT3, and inflammatory gene expression in

324   immune cell subsets will be crucial for our understanding of the molecular functions of FTO in
325   disease.
326

333

334   **Author contributions**
335   Conceptualization: M.J.M., M.T.S., N.S.G., and S.M.H. Investigation: M.J.M., M.T.S.,
336   N.S.G., and M.P. Formal analysis: M.J.M., M.T.S., K.A.M., N.S.G., and S.M.H. Software: K.A.M.,
337   N.S.G., and K.Y.S. Writing – original draft: M.J.M. and S.M.H. Writing – review and editing: M.J.M.,
338   M.T.S., K.A.M., N.S.G., K.Y.S., and S.M.H. Funding acquisition: S.M.H.
339

340   **Competing interests**
341   The authors have no competing interests to declare.
342

343   **Methods**
344   **Cell Lines.** Human hepatoma Huh7 cells and embryonic kidney 293T cells were grown in
345   Dulbecco's modification of Eagle's medium (DMEM; Mediatech) supplemented with 10% fetal
346   bovine serum (Thermo Fisher Scientific), 1X minimum essential medium non-essential amino
347   acids (Thermo Fisher Scientific), and 25 mM HEPES (Thermo Fisher Scientific) (cDMEM). The
348   identity of the Huh7 cells used in this study was verified by using the GenePrint STR kit (Promega)
349   (DNA Analysis Facility, Duke University, Durham, NC, USA). Huh7 cells were a gift of Dr. Michael
350   Gale Jr., and 293T cells (WT and PCIF1 KO) [20] were a gift of Dr. Eric Greer. All cell lines were
351   verified as mycoplasma free by the LookOut Mycoplasma PCR detection kit (Sigma).
352

353   **IFN-β and IL-6 Treatment.** All IFN-β (PBL Assay Science) and IL-6 (Sigma-Aldrich) treatments
354   were performed at a concentration of 50 units/mL and 50 ng/mL in cDMEM, respectively.
355

356   **Plasmids.** pcDNA3.1-FLAG-stm2585 (FLAG-SarA) and pcDNA3.1 empty vector plasmids [51]
357   were gifts of Dr. Dennis Ko (Duke).

358

359 **Transfection.** siRNAs directed against METTL3 (SI04317096), METTL14 (SI00459942), FTO

360 (SI04177530), STAT3 (M-003544-02) or non-targeting AllStars negative control siRNA (1027280)

361 were purchased from Qiagen or Dharmacon. All siRNA transfections were performed using the

362 Lipofectamine RNAiMax reagent (Invitrogen), according to manufacturer's instructions.

363 siMETTL3/14 co-transfections were performed at a ratio of 1:2 siMETTL3:siMETTL14. Cells were

364 transfected with 25 pmol of siRNA at a final concentration of 0.0125 μM. Media was changed 4

365 hours post-transfection, and cells were incubated for 36 hours post-transfection prior to each

366 experimental treatment. Plasmid transfections were performed with 1 μg of DNA per single well

367 of a 6-well plate using PEI MAX (Polysciences, INC.) according to the manufacturer's instructions.

368 Media was changed 4 hours post-transfection, and cells were incubated for 36 hours post-

369 transfection prior to each experimental treatment.

370

371 **Immunoblotting.** Cells were lysed in a modified radioimmunoprecipitation assay (RIPA) buffer

372 (10 mM Tris [pH 7.5], 150 mM NaCl, 0.5% sodium deoxycholate, and 1% Triton X-100)

373 supplemented with protease inhibitor cocktail (Sigma) and phosphatase inhibitor cocktail II

374 (Millipore), and post-nuclear lysates were harvested by centrifugation. Quantified protein

375 (between 5 and 15 μg) was added to a 4X SDS protein sample buffer (40% glycerol, 240 mM

376 Tris-HCl [pH 6.8], 8% SDS, 0.04% bromophenol blue, 5% beta-mercaptoethanol), resolved by

377 SDS/PAGE, and transferred to nitrocellulose membranes in a 25 mM Tris-192 mM glycine-0.01%

378 SDS buffer. Membranes were stained with Revert 700 total protein stain (LI-COR Biosciences),

379 then blocked in 3% bovine serum albumin. Membranes were incubated with primary antibodies

380 for 2 hours at room temperature or overnight at 4°C. After washing with PBS-T buffer (1× PBS,

381 0.05% Tween 20), membranes were incubated with species-specific horseradish peroxidase-

382 conjugated antibodies (Jackson ImmunoResearch, 1:5000) for 1 hour at room temperature,

383 followed by treatment of the membrane with Clarity enhanced chemiluminescence (Bio-Rad) and

384 imaging on an Odyssey Fc imaging system (LI-COR Biosciences). The following antibodies were

385 used for immunoblotting: mouse anti-IFITM1 (Proteintech 60074-1-Ig, 1:1000; recognizes IFITM1

386 but not IFITM2 or IFITM3 [52, 53]), rabbit anti-MX1 (Abcam ab207414, 1:1000), mouse anti-ISG15

387 (Santa Cruz sc-166755, 1:5000), rabbit anti-EIF2AK2 (Abcam ab32506, 1:1000), rabbit anti-

388 GBP1 (Abcam EPR8285), mouse anti-IFIT3 (Abcam ab76818), rabbit anti-METTL14 (Sigma

389 HPA038002, 1:2500), mouse anti-METTL3 (Abnova H00056339-B01P, 1:1000), rabbit anti-FTO

390 (Abcam EPR6895, 1:1000), mouse anti-FTO (Abcam ab92821, 1:2000), mouse anti-STAT3 (Cell

391 Signaling Technologies 9139S, 1:2000), rabbit anti-phospho-STAT3 (Cell Signaling

14

392   Technologies, 1:2000), anti-PCIF (Bethyl Laboratory, 1:1000), mouse anti-FLAG-HRP (Sigma

393   A8592, 1:5000).

394

395   **Quantification of Immunoblots.** Following imaging using the LI-COR Odyssey Fc, immunoblots

396   were quantified using ImageStudio Lite software, and raw values were normalized to total protein

397   (Revert 700 total protein stain) for each condition.

398

399   **RT-qPCR.** Total cellular RNA was extracted using the Qiagen RNeasy kit (Life Technologies) or

400   TRIzol extraction (Thermo Fisher Scientific). RNA was then reverse transcribed using the iScript

401   cDNA synthesis kit (Bio-Rad) as per the manufacturer's instructions. The resulting cDNA was

402   diluted 1:5 in nuclease-free H2O. RT-qPCR was performed in triplicate using the Power SYBR

403   Green PCR master mix (Thermo Fisher Scientific) and the Applied Biosystems Step One Plus or

404   QuantStudio 6 Flex RT-PCR systems. Primer sequences for RT-qPCR are listed in Table 1.

405

406   **Table 1:** RT-qPCR Primer Sequences.

Target	Forward Primer (5'-3')	Reverse Primer (5'-3')
GAPDH	AAGGTGAAGGTCGGAGTCAAC	GGGGTCATTGATGGCAACAATA
HPRT1	TGACACTGGCAAAACAATGCA	GGTCCTTTTCACCAGCAAGCT
CREBBP	CTCAGCTGTGACCTCATGGA	AGGTCGTAGTCCTCGCACAC
IFITM1	ACTAGTAGCCGCCCATAGCC	GCACGTGCACTTTATTGAATG
MX1	TTCAGCACCTGATGGCCTATC	TGGATGATCAAAGGGATGTGG
ISG15	GCGAACTCATCTTTGCCAGTA	CCAGCA TCTTCACCGTCAG
EIF2AK2	TCGCTGGTATCACTCGTCTG	GATTCTGAAGACCGCCAGAG
GBP1	GTGGAACGTGTGAAAGCTGA	CAACTGGACCCTGTCGTTCT
IFIT3	AGTCTAGTCACTTGGGGAAAC	ATAAATCTGAGCATCTGAGAGTC
CXCL10	AGCAGAGGAACCTCCAGTCT	ATGCAGGTACAGCGTACAGT

407

408   **Metabolic labeling of nascent transcripts with 4-sU.** siRNA-treated cells were pulsed with 4-

409   sU at a final concentration of 200 µM (-/+ IFN-β) for the indicated amount of time before harvest

410   in TRIzol and RNA extraction. Purification of newly transcribed, 4-sU labeled RNA was performed

411   as previously described [54]. Briefly, 50 µg of RNA were biotinylated in biotinylation buffer (10 mM

412   Tris-HCl pH 7.4, 1 mM EDTA, 20 ng/µl MTSEA Biotin-XX (Biotium)) for 30 minutes at room

413   temperature, shaking at 800 rpm. A phenol/chloroform extraction was performed, and RNA was

414   precipitated in isopropanol for 1 hour at -20°C. Following centrifugation for 20 minutes at 12000

415   X g at 4°C, RNA was resuspended, and 20% of each sample was taken for input samples. The

416   remaining RNA was then incubated with Streptavidin MyOne C1 Dynabeads (Thermo Fisher

417   Scientific), which were prewashed with 0.1M NaCl, in streptavidin binding buffer (final

418 concentration 5 mM Tris-HCl pH 7.4, 0.5 mM EDTA, 1M NaCl) for 30 minutes at room
419 temperature, shaking at 800 rpm. The supernatant containing unbound "pre-existing" RNA was
420 then collected, and the beads were washed 4X with wash buffer (100 mM Tris-HCl pH 7.4, 10
421 mM EDTA, 1M NaCl, 0.1% Tween-20), and each wash was collected. Two additional washes
422 were performed, and supernatant was discarded. To elute biotinylated RNA, 100 mM DTT (freshly
423 prepared) was added, and the supernatant was collected. This was repeated 3 times to collect all
424 labeled RNA. Finally, both the "pre-existing" and "newly transcribed" fractions were precipitated
425 in isopropanol for 1 hour at -20°C. Following centrifugation for 20 minutes at 12000 X g at 4°C,
426 RNA was resuspended, and cDNA was synthesized for each RNA fraction using the iScript cDNA
427 synthesis kit (BioRad). RT-qPCR was then performed for total and newly transcribed fractions
428 and used to determine the relative transcription rate of genes of interest, compared to GAPDH.
429

430 **RNA-seq.** Following siRNA treatment (36 hours), Huh7 cells seeded in 10-cm^2 plates were
431 stimulated with IFN-β or mock treated (8 hours), then harvested and RNA extraction was
432 performed using TRIzol reagent (Thermo Fisher Scientific). Samples were then treated with Turbo
433 DNase I (Thermo Fisher Scientific) according to manufacturer protocol and incubated at 37°C for
434 30 minutes, followed by phenol/chloroform extraction and ethanol precipitation overnight. RNA
435 concentrations were then normalized. Sequencing libraries were prepared using the KAPA
436 Stranded mRNA-Seq Kit (Roche) and sequenced on an Illumina HiSeq 4000 with 100 bp paired-
437 end reads by the Duke University Center for Genomic and Computational Biology.
438   Reads were aligned using Salmon [55] to the human reference transcriptome using default
439 parameters (hg19). Differential gene expression between infected and uninfected samples was
440 compared using DESeq2 [56]. Gene ontology analyses were generated using the PANTHER
441 Classification System's statistical enrichment test with gene symbols and fold change values [57].
442 The heatmaps were generated using Python scripts. We compared the effects of IFN-B and mock
443 treatment in cells transfected with siCTRL to determine the most highly induced interferon
444 stimulated genes based on adjusted P-value < 0.01 and a basemean > 50. To determine the
445 effect of IFN-β treatment with FTO depletion, the log-transformed adjusted P-value and fold
446 changes of the previously determined highly induced genes were plotted from the IFN-β and mock
447 treatments using Python scripts. Heatmaps of the 50 most induced ISGs and pro-inflammatory
448 chemokines and cytokines were generated using Python scripts.
449

450 **Data Availability.** All raw data from RNA-seq are available through GEO (accession number:
451 GSE180663).
452

453 **Code Availability.** All RNA-seq analysis scripts are open-source or online on Github

454 (https://github.com/kristen-a-murphy/McFadden_siFTO_RNA-seq).

455

456 **Supplemental Information**

457 Table S1: RNA-seq analysis of gene expression changes following IFN-β treatment and FTO

458 depletion.

459 • Table S1.1: siCTRL IFN / siCTRL Mock

460 • Table S1.2: siFTO IFN / siCTRL IFN

461 • Table S1.3: siFTO Mock / siCTRL Mock

462 Table S2: Gene Ontology analysis of RNA-seq data.

463 • Table S2.1: Enriched GO categories for differentially expressed genes (siFTO Mock /

464 siCTRL Mock)

465 • Table S2.2: Enriched GO categories for differentially expressed genes (siFTO IFN /

466 siCTRL IFN)

467

468

References

[1] Schoggins JW, Wilson SJ, Panis M, Murphy MY, Jones CT, Bieniasz P, et al. A diverse range of gene products are effectors of the type I interferon antiviral response. Nature. 2011;472:481-5.

[2] Stark GR, Darnell JE, Jr. The JAK-STAT pathway at twenty. Immunity. 2012;36:503-14.

[3] Schneider WM, Chevillotte MD, Rice CM. Interferon-stimulated genes: a complex web of host defenses. Annu Rev Immunol. 2014;32:513-45.

[4] Tsai MH, Pai LM, Lee CK. Fine-Tuning of Type I Interferon Response by STAT3. Front Immunol. 2019;10:1448.

[5] McFadden MJ, McIntyre ABR, Mourelatos H, Abell NS, Gokhale NS, Ipas H, et al. Post-transcriptional regulation of antiviral gene expression by N6-methyladenosine. Cell Rep. 2021;34:108798.

[6] Frayling TM, Timpson NJ, Weedon MN, Zeggini E, Freathy RM, Lindgren CM, et al. A common variant in the FTO gene is associated with body mass index and predisposes to childhood and adult obesity. Science. 2007;316:889-94.

[7] Dina C, Meyre D, Gallina S, Durand E, Körner A, Jacobson P, et al. Variation in FTO contributes to childhood obesity and severe adult obesity. Nat Genet. 2007;39:724-6.

[8] Speliotes EK, Willer CJ, Berndt SI, Monda KL, Thorleifsson G, Jackson AU, et al. Association analyses of 249,796 individuals reveal 18 new loci associated with body mass index. Nat Genet. 2010;42:937-48.

[9] Olza J, Ruperez AI, Gil-Campos M, Leis R, Fernandez-Orth D, Tojo R, et al. Influence of FTO variants on obesity, inflammation and cardiovascular disease risk biomarkers in Spanish children: a case-control multicentre study. BMC Med Genet. 2013;14:123.

[10] Boissel S, Reish O, Proulx K, Kawagoe-Takaki H, Sedgwick B, Yeo GS, et al. Loss-of-function mutation in the dioxygenase-encoding FTO gene causes severe growth retardation and multiple malformations. Am J Hum Genet. 2009;85:106-11.

[11] Gerken T, Girard CA, Tung YC, Webby CJ, Saudek V, Hewitson KS, et al. The obesity-associated FTO gene encodes a 2-oxoglutarate-dependent nucleic acid demethylase. Science. 2007;318:1469-72.

[12] Jia G, Fu Y, Zhao X, Dai Q, Zheng G, Yang Y, et al. N6-methyladenosine in nuclear RNA is a major substrate of the obesity-associated FTO. Nat Chem Biol. 2011;7:885-7.

[13] Zheng G, Dahl JA, Niu Y, Fedorcsak P, Huang CM, Li CJ, et al. ALKBH5 is a mammalian RNA demethylase that impacts RNA metabolism and mouse fertility. Mol Cell. 2013;49:18-29.

[14] Mauer J, Luo X, Blanjoie A, Jiao X, Grozhik AV, Patil DP, et al. Reversible methylation of m(6)A(m) in the 5' cap controls mRNA stability. Nature. 2017;541:371-5.

[15] Liu J, Yue Y, Han D, Wang X, Fu Y, Zhang L, et al. A METTL3-METTL14 complex mediates mammalian nuclear RNA N6-adenosine methylation. Nat Chem Biol. 2014;10:93-5.

506   [16] Wang X, Lu Z, Gomez A, Hon GC, Yue Y, Han D, et al. N6-methyladenosine-dependent
507   regulation of messenger RNA stability. Nature. 2014;505:117-20.

508   [17] Wang X, Zhao BS, Roundtree IA, Lu Z, Han D, Ma H, et al. N(6)-methyladenosine
509   Modulates Messenger RNA Translation Efficiency. Cell. 2015;161:1388-99.

510   [18] Shi H, Wang X, Lu Z, Zhao BS, Ma H, Hsu PJ, et al. YTHDF3 facilitates translation and
511   decay of N(6)-methyladenosine-modified RNA. Cell Res. 2017;27:315-28.

512   [19] He L, Li H, Wu A, Peng Y, Shu G, Yin G. Functions of N6-methyladenosine and its role in
513   cancer. Mol Cancer. 2019;18:176.

514   [20] Boulias K, Toczydłowska-Socha D, Hawley BR, Liberman N, Takashima K, Zaccara S, et
515   al. Identification of the m(6)Am Methyltransferase PCIF1 Reveals the Location and Functions of
516   m(6)Am in the Transcriptome. Mol Cell. 2019;75:631-43.e8.

517   [21] Akichika S, Hirano S, Shichino Y, Suzuki T, Nishimasu H, Ishitani R, et al. Cap-specific
518   terminal N (6)-methylation of RNA by an RNA polymerase II-associated methyltransferase.
519   Science. 2019;363.

520   [22] Sendinc E, Valle-Garcia D, Dhall A, Chen H, Henriques T, Navarrete-Perea J, et al. PCIF1
521   Catalyzes m6Am mRNA Methylation to Regulate Gene Expression. Mol Cell. 2019;75:620-
522   30.e9.

523   [23] Li L, Zang L, Zhang F, Chen J, Shen H, Shu L, et al. Fat mass and obesity-associated
524   (FTO) protein regulates adult neurogenesis. Hum Mol Genet. 2017;26:2398-411.

525   [24] Hess ME, Hess S, Meyer KD, Verhagen LA, Koch L, Brönneke HS, et al. The fat mass and
526   obesity associated gene (Fto) regulates activity of the dopaminergic midbrain circuitry. Nat
527   Neurosci. 2013;16:1042-8.

528   [25] Karra E, O'Daly OG, Choudhury AI, Yousseif A, Millership S, Neary MT, et al. A link
529   between FTO, ghrelin, and impaired brain food-cue responsivity. J Clin Invest. 2013;123:3539-
530   51.

531   [26] Zhao X, Yang Y, Sun BF, Shi Y, Yang X, Xiao W, et al. FTO-dependent demethylation of
532   N6-methyladenosine regulates mRNA splicing and is required for adipogenesis. Cell Res.
533   2014;24:1403-19.

534   [27] Li Z, Weng H, Su R, Weng X, Zuo Z, Li C, et al. FTO Plays an Oncogenic Role in Acute
535   Myeloid Leukemia as a N(6)-Methyladenosine RNA Demethylase. Cancer Cell. 2017;31:127-41.

536   [28] Yang S, Wei J, Cui YH, Park G, Shah P, Deng Y, et al. m(6)A mRNA demethylase FTO
537   regulates melanoma tumorigenicity and response to anti-PD-1 blockade. Nat Commun.
538   2019;10:2782.

539   [29] Williams GD, Gokhale NS, Horner SM. Regulation of Viral Infection by the RNA
540   Modification N6-Methyladenosine. Annu Rev Virol. 2019;6:235-53.

541   [30] Heinrich PC, Behrmann I, Haan S, Hermanns HM, Müller-Newen G, Schaper F. Principles
542   of interleukin (IL)-6-type cytokine signalling and its regulation. Biochem J. 2003;374:1-20.

543   [31] Gibbs KD, Washington EJ, Jaslow SL, Bourgeois JS, Foster MW, Guo R, et al. The
544   Salmonella Secreted Effector SarA/SteE Mimics Cytokine Receptor Signaling to Activate
545   STAT3. Cell Host Microbe. 2020;27:129-39.e4.

546   [32] Turner MD, Nedjai B, Hurst T, Pennington DJ. Cytokines and chemokines: At the
547   crossroads of cell signalling and inflammatory disease. Biochim Biophys Acta. 2014;1843:2563-
548   82.

549   [33] Bravard A, Vial G, Chauvin MA, Rouillé Y, Bailleul B, Vidal H, et al. FTO contributes to
550   hepatic metabolism regulation through regulation of leptin action and STAT3 signalling in liver.
551   Cell Commun Signal. 2014;12:4.

552   [34] Carpenter RL, Lo HW. STAT3 Target Genes Relevant to Human Cancers. Cancers (Basel).
553   2014;6:897-925.

554   [35] Yang CH, Wei L, Pfeffer SR, Du Z, Murti A, Valentine WJ, et al. Identification of CXCL11 as
555   a STAT3-dependent gene induced by IFN. J Immunol. 2007;178:986-92.

556   [36] Minami M, Inoue M, Wei S, Takeda K, Matsumoto M, Kishimoto T, et al. STAT3 activation
557   is a critical step in gp130-mediated terminal differentiation and growth arrest of a myeloid cell
558   line. Proc Natl Acad Sci U S A. 1996;93:3963-6.

559   [37] Lin S, Choe J, Du P, Triboulet R, Gregory RI. The m(6)A Methyltransferase METTL3
560   Promotes Translation in Human Cancer Cells. Mol Cell. 2016;62:335-45.

561   [38] Gimeno R, Lee CK, Schindler C, Levy DE. Stat1 and Stat2 but not Stat3 arbitrate
562   contradictory growth signals elicited by alpha/beta interferon in T lymphocytes. Mol Cell Biol.
563   2005;25:5456-65.

564   [39] Horvath CM, Darnell JE, Jr. The antiviral state induced by alpha interferon and gamma
565   interferon requires transcriptionally active Stat1 protein. J Virol. 1996;70:647-50.

566   [40] Nakayamada S, Poholek AC, Lu KT, Takahashi H, Kato M, Iwata S, et al. Type I IFN
567   induces binding of STAT1 to Bcl6: divergent roles of STAT family transcription factors in the T
568   follicular helper cell genetic program. J Immunol. 2014;192:2156-66.

569   [41] Ho HH, Ivashkiv LB. Role of STAT3 in type I interferon responses. Negative regulation of
570   STAT1-dependent inflammatory gene activation. J Biol Chem. 2006;281:14111-8.

571   [42] Tsai MH, Lee CK. STAT3 Cooperates With Phospholipid Scramblase 2 to Suppress Type I
572   Interferon Response. Front Immunol. 2018;9:1886.

573   [43] Qin H, Niyongere SA, Lee SJ, Baker BJ, Benveniste EN. Expression and functional
574   significance of SOCS-1 and SOCS-3 in astrocytes. J Immunol. 2008;181:3167-76.

575   [44] Croker BA, Kiu H, Nicholson SE. SOCS regulation of the JAK/STAT signalling pathway.
576   Semin Cell Dev Biol. 2008;19:414-22.

577   [45] Wu R, Guo G, Bi Z, Liu Y, Zhao Y, Chen N, et al. m(6)A methylation modulates
578   adipogenesis through JAK2-STAT3-C/EBPβ signaling. Biochim Biophys Acta Gene Regul
579   Mech. 2019;1862:796-806.

580   [46] Hirano T. Interleukin 6 and its receptor: ten years later. Int Rev Immunol. 1998;16:249-84.

581   [47] Parri E, Kuusanmäki H, van Adrichem AJ, Kaustio M, Wennerberg K. Identification of novel
582   regulators of STAT3 activity. PLoS One. 2020;15:e0230819.

583   [48] McFadden MJ, Horner SM. N(6)-Methyladenosine Regulates Host Responses to Viral
584   Infection. Trends Biochem Sci. 2021;46:366-77.

585   [49] Tartell MA, Boulias K, Hoffmann GB, Bloyet L-M, Greer EL, Whelan SPJ. Methylation of
586   viral mRNA cap structures by PCIF1 attenuates the antiviral activity of interferon-β. Proceedings
587   of the National Academy of Sciences. 2021;118.

588   [50] Rong ZX, Li Z, He JJ, Liu LY, Ren XX, Gao J, et al. Downregulation of Fat Mass and
589   Obesity Associated (FTO) Promotes the Progression of Intrahepatic Cholangiocarcinoma. Front
590   Oncol. 2019;9:369.

591   [51] Jaslow SL, Gibbs KD, Fricke WF, Wang L, Pittman KJ, Mammel MK, et al. Salmonella
592   Activation of STAT3 Signaling by SarA Effector Promotes Intracellular Replication and
593   Production of IL-10. Cell Rep. 2018;23:3525-36.

594   [52] Xie M, Xuan B, Shan J, Pan D, Sun Y, Shan Z, et al. Human cytomegalovirus exploits
595   interferon-induced transmembrane proteins to facilitate morphogenesis of the virion assembly
596   compartment. J Virol. 2015;89:3049-61.

597   [53] Shi G, Ozog S, Torbett BE, Compton AA. mTOR inhibitors lower an intrinsic barrier to virus
598   infection mediated by IFITM3. Proc Natl Acad Sci U S A. 2018;115:E10069-e78.

599   [54] Dölken L, Ruzsics Z, Rädle B, Friedel CC, Zimmer R, Mages J, et al. High-resolution gene
600   expression profiling for simultaneous kinetic parameter analysis of RNA synthesis and decay.
601   RNA. 2008;14:1959-72.

602   [55] Patro R, Duggal G, Love MI, Irizarry RA, Kingsford C. Salmon provides fast and bias-aware
603   quantification of transcript expression. Nat Methods. 2017;14:417-9.

604   [56] Love MI, Huber W, Anders S. Moderated estimation of fold change and dispersion for RNA-
605   seq data with DESeq2. Genome Biol. 2014;15:550.

606   [57] Mi H, Ebert D, Muruganujan A, Mills C, Albou LP, Mushayamaha T, et al. PANTHER
607   version 16: a revised family classification, tree-based classification tool, enhancer regions and
608   extensive API. Nucleic Acids Res. 2021;49:D394-d403.

609

610